



UNIVERSITY OF LEEDS

This is a repository copy of *An assessment of landform composition and functioning with the first proglacial systems dataset of the central European Alps*.

White Rose Research Online URL for this paper:
<http://eprints.whiterose.ac.uk/135754/>

Version: Accepted Version

Article:

Carrivick, JL orcid.org/0000-0002-9286-5348, Heckmann, T, Turner, A orcid.org/0000-0002-6098-6313 et al. (1 more author) (2018) An assessment of landform composition and functioning with the first proglacial systems dataset of the central European Alps. *Geomorphology*, 321. pp. 117-128. ISSN 0169-555X

<https://doi.org/10.1016/j.geomorph.2018.08.030>

© 2018 Elsevier B.V. This manuscript version is made available under the CC-BY-NC-ND 4.0 license <http://creativecommons.org/licenses/by-nc-nd/4.0/>.

Reuse

This article is distributed under the terms of the Creative Commons Attribution-NonCommercial-NoDerivs (CC BY-NC-ND) licence. This licence only allows you to download this work and share it with others as long as you credit the authors, but you can't change the article in any way or use it commercially. More information and the full terms of the licence here: <https://creativecommons.org/licenses/>

Takedown

If you consider content in White Rose Research Online to be in breach of UK law, please notify us by emailing eprints@whiterose.ac.uk including the URL of the record and the reason for the withdrawal request.



eprints@whiterose.ac.uk
<https://eprints.whiterose.ac.uk/>

An assessment of landform composition and functioning with the first proglacial systems dataset of the central European Alps

Jonathan L. Carrivick¹, Tobias Heckmann², Andy Turner¹, Mauro Fischer³

¹School of Geography, University of Leeds, Woodhouse Lane, Leeds, West Yorkshire, LS2 9JT, UK.

²Physical Geography, Catholic University of Eichstaett-Ingolstadt, Germany.

³ Institute of Geography, University of Bern, Hallerstrasse 12, 3012 Bern, Switzerland.

correspondence to:
Dr. Jonathan Carrivick,
Email: j.l.carrivick@leeds.ac.uk
Tel.: 0113 343 3324

ABSTRACT

Proglacial systems are enlarging as glacier masses decline. They are in a transitory state from glacier-dominated to hillslope and fluvially-dominated geomorphological processes. They are a very important meltwater, sediment and solute source. This study makes the first quantitative, systematic and regional assessment of landform composition and functioning within proglacial systems that have developed in the short term since the Little Ice Age (LIA). Proglacial system extent was thus defined as the area between the LIA moraine ridges and the contemporary glacier. We achieved this assessment via a series of topographic analyses of 10 m resolution digital elevation models (DEMs) covering the central European Alps, specifically of Austria and Switzerland. Across the 2812 proglacial systems that have a combined area of 933 km², the mean proportional area of each proglacial system that is directly affected by glacial meltwater is 37 %. However, there are examples where there is no glacial meltwater influence whatsoever due to complete disappearance of glaciers since the LIA, and there are examples where > 90% of the proglacial area is probably affected by glacial meltwater. In all of the major drainage basins; the Inn, Drava, Venetian Coast, Po, Rhine, Rhone and Danube, the proportions of the combined land area belonging to each landform class is remarkably similar, with > 10 % fluvial, ~35 % alluvial and debris fans, ~50 % moraine ridges and talus/scree, and ~ 10 % bedrock, which will be very helpful for considering estimates of regional sediment yield and denudation rates. We find groupings of the relationship between proglacial system hypsometric index and lithology, and of a slope threshold discriminating between hillslope and fluvial-dominated terrain, both of which we interpret to be due to grain size. We estimate of contemporary total volume loss from all of these proglacial systems of 44 M m³a⁻¹, which equates to a mean of 0.3 mm.a⁻¹ contemporary surface lowering. Overall, these first quantifications of proglacial landform and landscape evolution will be an important basis for inter- and intra-catchment considerations of climate

40 change effects on proglacial systems such as land stability, and changing water, sediment and
41 solute source fluxes. Our datasets are made freely available.

42

43 **KEYWORDS**

44 proglacial; glacier; landform; meltwater; landscape evolution; hillslope; fluvial

45

46 **HIGHLIGHTS**

47 • Delineation of 2812 proglacial systems in central European Alps of total 933 km².

48 • Glacier meltwater and landform coverage spatially discriminated for each system.

49 • Lithological control evident in slope threshold – contributing area analysis.

50 • First order estimate of total contemporary volume loss = 44 M m³a⁻¹.

51

52 **1. INTRODUCTION**

53 Proglacial systems are amongst the most rapidly changing landscapes on Earth. They are
54 progressively increasing in areal extent, and arguably also in instability due to ongoing
55 effects of climate change on glaciers, permafrost and consequent hillslope and fluvial
56 processes (Ballantyne, 2002; Carrivick and Heckmann, 2017). They are a source of water,
57 sediment, solutes (WSS) and hazardous geophysical phenomena, particularly landslides and
58 glacier outburst floods (GLOFs) (e.g. Carrivick and Tweed, 2013). WSS fluxes dictate alpine
59 hillslope and river channel stability, water thermal and chemical regime, biological
60 communities (fish, invertebrates, plants, algae), and ecosystem functions that influence water
61 quality (nutrient and carbon cycling). Proglacial system geomorphological composition and
62 functioning and landscape evolution are therefore of great importance for natural
63 environmental systems and for human activity. Furthermore, alpine proglacial systems in
64 both the European Alps and globally have influence on human and natural systems far
65 beyond the alpine zone. For example, there are 14 million people living in the European
66 alpine arc (Litschauer, 2014) and there are several billion people directly dependent on water
67 from alpine rivers globally. Across Europe, alpine river tributaries contribute up to eight
68 times the water discharge that might be expected given their basin size and thus have been
69 termed the ‘water towers of Europe’ (EEA, 2009; Huss, 2011).

70

71 Proglacial systems are transitioning from being dominated by glacial processes to being more
72 influenced by paraglacial hillslope and fluvial processes (Church and Ryder, 1972;

73 Ballantyne, 2002; Carrivick and Heckmann, 2017). A transitory state implies intense
74 hydrological, geomorphological and ecological dynamics (c.f. Heckmann et al., 2015;
75 Micheletti and Lane, 2017; Delaney et al., 2017; Heckmann and Morche, in press). However,
76 identifying WSS patterns due to these environmental transition(s) is not straight-forward due
77 to spatio-temporal variability and non-linear and stochastic relationships (Bennett et al.,
78 2014). Furthermore, whilst paraglacial activity is generally considered as a set of earth
79 surface processes that are dominant during the transition time period (Carrivick and
80 Heckmann, 2017), changes in hillslope and channel composition or landforms and sediments,
81 and functioning such as connectivity, can alter the relative importance of these hillslope and
82 fluvial processes in space and time (Bennett et al., 2014; Lane et al., 2017).

83

84 Despite the importance of understanding WSS production, pathways and effluxes, studies of
85 geomorphological composition and functioning within proglacial systems have been few and
86 spatio-temporally disparate. Indeed, geomorphological mapping within proglacial systems
87 tends to be conducted either as a basis for field monitoring of water and sediment fluxes (e.g.
88 Beylich et al., 2017), or as a preliminary step towards making targeted close-range field
89 surveys of topographic changes (e.g. Carrivick et al., 2013; Kociuba, 2016). There have been
90 no quantitative efforts to evaluate the geomorphological composition of proglacial systems
91 across a region, nor to evaluate spatial coverage of major geomorphological processes across
92 a mountain range scale region, nor to evaluate likely sediment sources, pathways and sinks
93 within proglacial systems across a region. These three efforts are necessary precursors to
94 regionalising or upscaling field measurements, and more specifically for making quantitative
95 estimates of volume and mass changes within (and exports from) proglacial systems.

96

97 This study therefore aims to make the first comprehensive quantitative, systematic and
98 regional assessment of landform composition and functioning within proglacial systems. We
99 focus on the central European Alps region due to that region having readily-available data
100 and because we have (published) knowledge of some of the catchments in that region, but we
101 advocate the relevance of this work globally.

102

103 2. STUDY AREAS, DATASETS AND METHODS

104

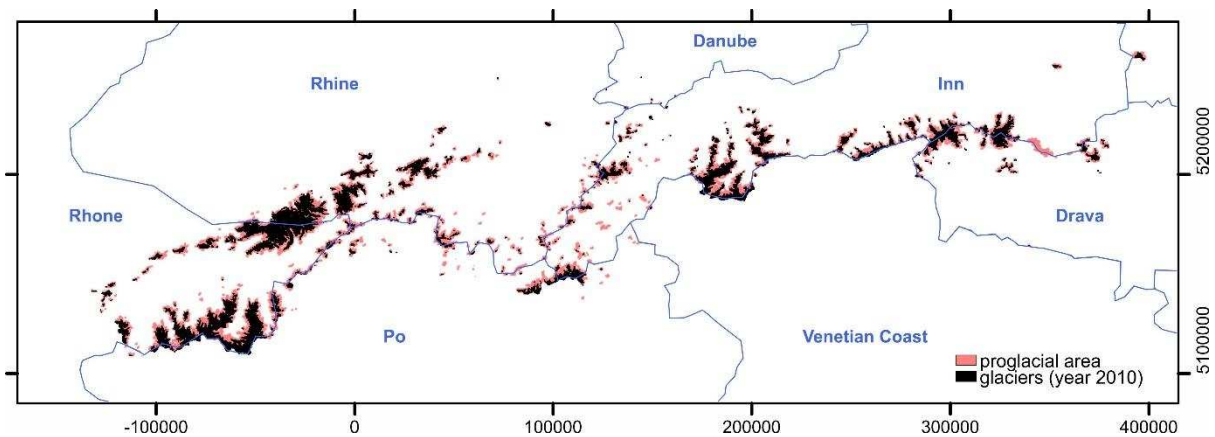
105 2.1 Proglacial zone definition

106 Proglacial systems across the central European Alps analysed in this study are situated in both
 107 Austria and Switzerland due to both of those countries having high-resolution (10 m grid cell
 108 size or less) seamless digital data availability. Austria glacier outlines for both the Little Ice
 109 Age (LIA) and for the contemporary situation were obtained from Fischer et al. (2015a), Groß
 110 and Patzelt (2015) and Glaziologie Österreich (2016). A 10 m grid cell size DEM of Austria
 111 that had been down-sampled from airborne laser scanner (ALS) data was obtained via Daten
 112 Österreichs (2016).

113

114 Swiss glacier outlines for both the LIA considered those of Maisch (2000). For the
 115 contemporary (year 2010) situation they were obtained by manual digitization of high-
 116 resolution (0.25 m) aerial orthophotographs acquired between 2008 and 2011 (Fischer et al.,
 117 2014, 2015b). High-resolution topographic data for Switzerland comprising a 2 m grid cell
 118 size, down-sampled to 10 m grid cell size for this study to be comparable to the Austria Digital
 119 Elevation Model (DEM), was derived from Airborne Laser Scanning (ALS) as published by
 120 Fischer et al. (2014, 2015b).

121



122

123 **Figure 1. Spatial coverage of glaciers and proglacial systems across central Europe**
 124 **(Austria and Switzerland) with major drainage basin boundaries (watersheds). Grid**
 125 **coordinates (metres) are projected in UTM zone 33N.**
 126

127 Proglacial systems across the central European Alps (Fig. 1) were defined automatically by
 128 subtracting modern glacier outlines from LIA glacier outlines after Carrivick et al., (accepted).
 129 This simple calculation produced a proglacial system extent or boundary, which is necessary
 130 for spatial analyses, and a system area (spatial size). In order to minimise misidentifications
 131 and extraneous parts of proglacial systems (such as where: (i) some glaciers have reduced in
 132 width at relatively high elevations; (ii) some glaciers have reduced in ice extent on plateaux or
 133 on cols as a result of fragmentation or disintegration; and, (iii) portions of the landscape

134 presently in transition between ice-marginal and proglacial regimes), we specified a 100 m
 135 buffer around the modern outlines and excluded this area from our analyses.

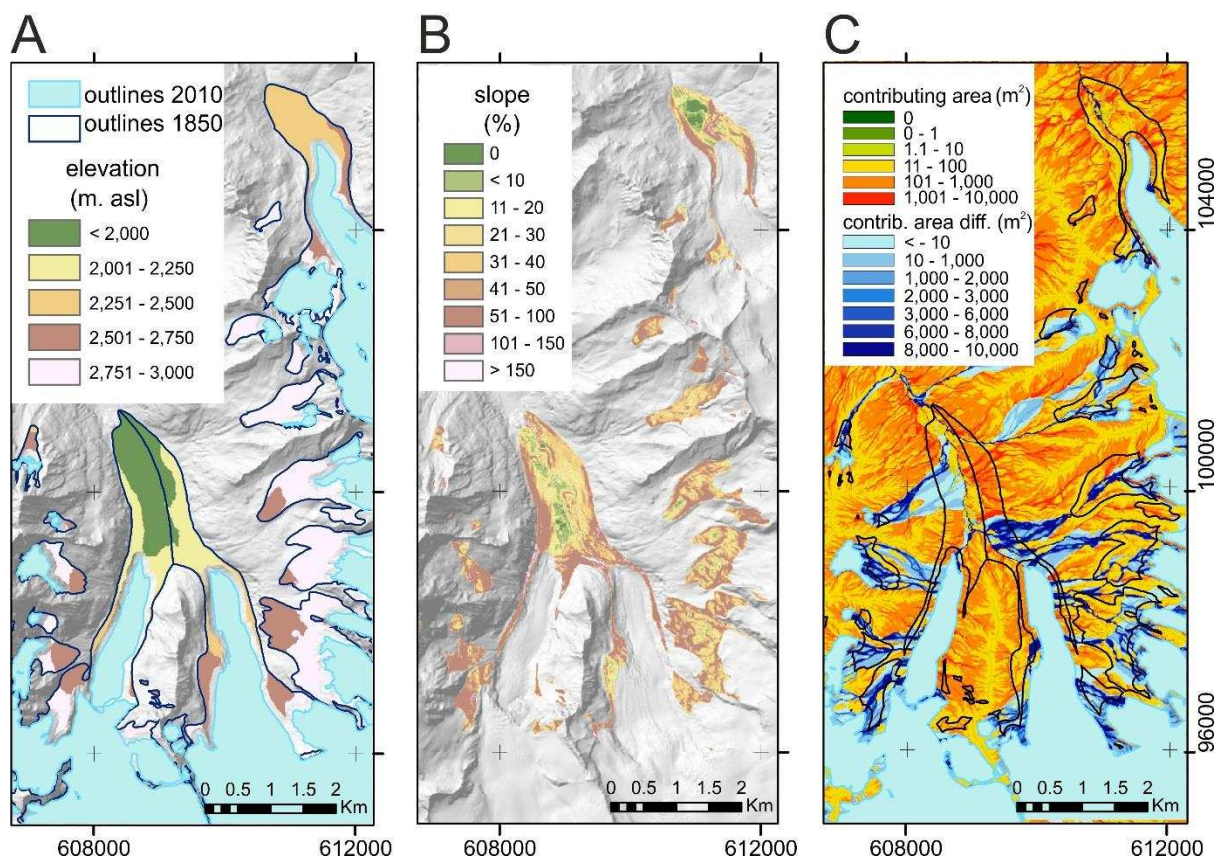
136

137 Geological data was sourced from the International Geological Map of Europe (Asch, 2003;
 138 IGME, 2016) and chosen over national level datasets so as to give consistency in mapping
 139 and terminology as well as a general-level classification suitable for the regional-scale
 140 analysis of this paper.

141

142 With consideration of future use of our results for understanding WSS fluxes from proglacial
 143 systems and especially of those transmitted downstream where they affect local populations,
 144 hydropower and communications infrastructure, and agriculture we discriminate by major
 145 central European drainage basin. These outlines (watersheds) were sourced from the Global
 146 Runoff Data Centre (GRDC) www.grdc.de.

147



148

149

150 **Figure 2. Example of the spatial discrimination of proglacial systems using glacier**
 151 **outlines from the LIA ‘year 1850’ (Maisch, 2000) and from the present ‘year 2010’ (A),**
 152 **of categories of slope in these systems (B) and of contributing area analysis (C), in this**
 153 **case for the Glacier du Mont Miné and Glacier de Ferpécle area in Switzerland. Shades**

154 **of blue in panel 1C can be considered to represent a ‘likelihood’ of that grid cell**
155 **receiving glacial meltwater runoff, being calculated per grid cell as the difference**
156 **between grids of contributing area with and without glaciers. Grid coordinates are**
157 **projected in CH1903_LV03.**
158

159 **2.2 Spatial discrimination of major geomorphological process domains**

160 In a first-order classification of proglacial systems based on their topography, we not only
161 calculated statistics of elevations (Fig. 2A) and slopes (Fig. 2B) of all grid cells within each
162 proglacial system, but also the hypsometric index of each as categorised following the Jiskoot
163 et al. (2009) approach where very top heavy hypsometric values indicate much more area at
164 high elevation than at low, and very bottom heavy hypsometric values indicate much more
165 area at low elevation than at high.

166
167 Our spatial discrimination of major geomorphological process domains was achieved in four
168 workflow stages, and was in terms of grid cells that are either predominantly influenced by
169 glacier meltwater, other fluvial (fluid flow) processes, or grid cells that are dominated by
170 hillslope (mostly gravitational) processes.

171
172 Firstly, slope grids (Fig. 2B) were computed and the cell values extracted for each proglacial
173 zone. Secondly, contributing area was determined per grid cell via the D-Infinity flow
174 direction and contributing area algorithms (Tarboton, 1997), as available in the TauDEM
175 (2016) set of tools. These algorithms were chosen to recognise the likelihood of braided river
176 networks in proglacial systems where local slopes are shallow. Contributing area calculations
177 assume that (runoff) contributing area correlates with water discharge. Thus they are not valid
178 for grid cells that might receive runoff from a glacier where discharge is driven by melt and
179 often with significant temporary storage. We therefore differenced grids of contributing area
180 with and without glacier surfaces in them. This calculation discriminated grid cells that
181 cannot receive runoff from glaciers, as coloured greens and reds in figure 2C, versus grid
182 cells that probably do receive runoff from glaciers, as coloured shades of blue in figure 2C.
183 This calculation of the spatial influence of glacial meltwater runoff does not consider flood
184 inundation extent, and we realise flooding is a regular phenomenon in proglacial systems, nor
185 (non-glacial) valley side tributaries.

186
187 After excluding all glacier-meltwater influenced grid cells, we thirdly fitted a polynomial
188 curve with varying numbers of parameters i.e. those of the form:

$$189 \quad Y = a*(X^2) + b*(X) + c \quad (1)$$

190 where Y = log contributing area, and X = log slope, was fitted to the scatterplot of points of
 191 log slope – log contributing area for each proglacial zone using an algorithm provided in the
 192 Apache Commons Math library ([https://commons.apache.org/proper/commons-](https://commons.apache.org/proper/commons-math/userguide/fitting.html)
 193 [math/userguide/fitting.html](https://commons.apache.org/proper/commons-math/userguide/fitting.html)). For proglacial systems with more than 10 data points and for
 194 fitted curves with an identifiable maximum value, the corresponding log slope (X) value was
 195 extracted. The automated implementation of this model was via bespoke Java programs
 196 which we have made open source and for which we utilised some third party open source
 197 libraries as available via: <https://github.com/agdturner/FluvioGlacial>.
 198 Fourthly and finally, conversion of this log percent slope to a degrees slope enabled mapping
 199 and calculation of the percentage area of each proglacial zone that is apparently dominated by
 200 either fluvial or hillslope processes.

201

202 The percentage area of each proglacial zone dominated by glacial meltwater was calculated
 203 similarly, by converting the difference in contributing area (Fig. 2C) to a binary 1 =
 204 difference, 0 = no difference, then summing the number of grid cells with a difference and
 205 calculating the area of these as a proportion of the total proglacial zone area.

206

207 **2.3 Segmentation of major landform types**

208 In order to estimate the proportion of different landform types associated with different
 209 geomorphological processes, we analysed the probability density function (PDF) of slope as
 210 described by Loye et al. (2009). The method assumes slope to be normally distributed on
 211 characteristic landform types, and aims at decomposing the observed slope PDF into a user-
 212 specified number of normal distributions. The intersections of the resulting PDFs can then be
 213 used to discriminate the pertaining landform types. Unlike Loye et al. (2009), we applied the
 214 expectation-maximisation algorithm implemented in the R package mixtools (Benaglia et al.,
 215 2009; Heckmann et al., 2016) to the slope PDF of a sample ($n=25000$). We limited this
 216 sample to a subarea of the countrywide DEM10, namely to the area covering the proglacial
 217 systems plus a 200 m buffer to include adjacent rockwalls, and with glacier-covered areas
 218 masked.

219

220 Figure 3A illustrates that the PDFs inferred from the 30 samples are more and more
 221 consistent with increasing mode; the largest scatter is evident for the “floodplain” class, while
 222 the PDFs representing rockwalls are all very similar. Accordingly, the range of possible

223 intersections of the single landform type PDFs is wider for T1 and T2, and quite narrow for
224 T3. Depending on the alpine morphotectonic unit, Loye et al. (2009) reported T3 in the range
225 46° to 54° ; intersections at T1 and T2 were not explicitly reported (due to the focus of the
226 paper), but can be extracted from their diagrams: $T1=8^{\circ}$ to 13° , $T2 = 21^{\circ}$ to 26° . Note that
227 Loye et al. (2009) used a one metre cell size DEM, so the values of slope are expected to be
228 higher than those computed from our ten metre cell size DEM.

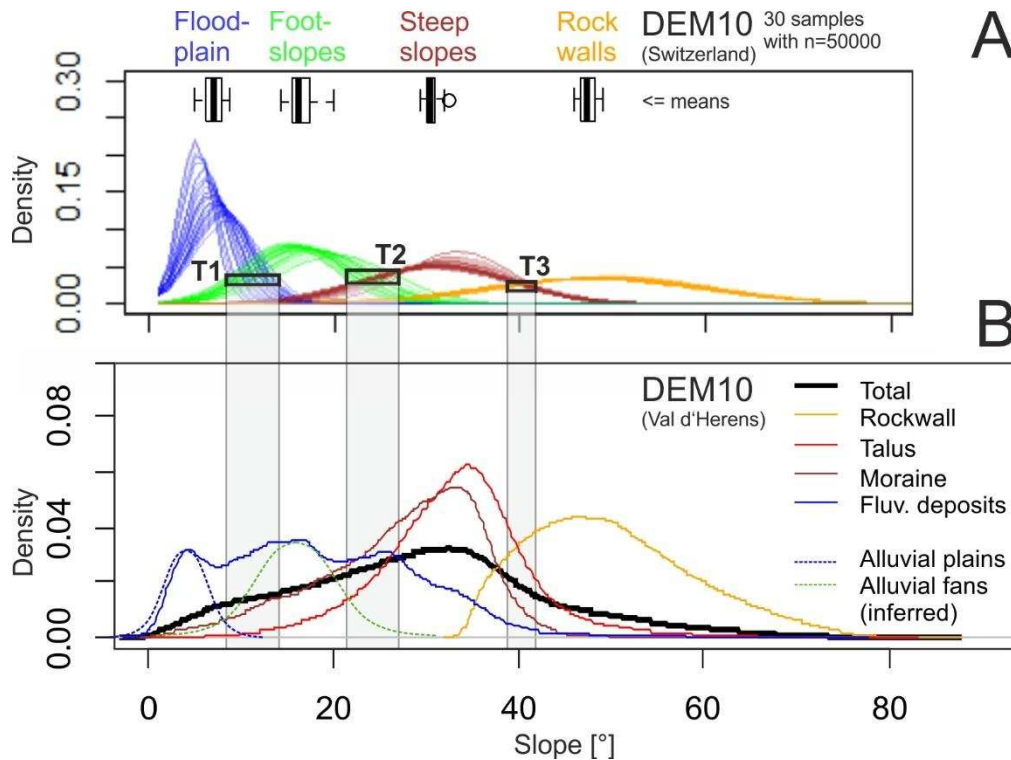
229

230 In order to validate the choice of intersections between each probabilistic group of slope
231 values, we analysed a 10 m cell size DEM of part of the Val d'Hérens (Switzerland), for
232 which Lambiel et al. (2016) have published a digital geomorphological map. We used the
233 polygons of selected landform types to extract the associated PDFs of slope from the DEM
234 (Figure 3B) and we found that the total slope PDF of the Val d'Hérens (thick black curve in
235 Figure 3B) was representative of the slope PDF of proglacial systems that we investigated in
236 the Austrian and Swiss DEMs.

237

238 Regarding the intersections of slope PDFs of different landform types, T3 appears to be
239 consistent with the intersections of the rockwall PDF with the PDFs of "talus" and
240 "moraine". The slope PDF of "fluvial deposits" in the map is multimodal, probably
241 accounting for floodplains, terraces and alluvial cones of different gradient; therefore, two
242 normal distributions have been fitted visually (the blue and green dashed curves) to the first
243 two modes of the "fluvial deposits" PDF. They intersect with each other in the range of T1
244 (upper panel), and with the "talus" PDF in the range of T2. Based on these observations, we
245 regard our classification as sufficient and set the intersections for discriminating probabilistic
246 slope groups at (a) 7.5° , (b) 18° and (c) 42° .

247



248

249

250 **Figure 3. A: Normal distributions of slope for four landform types generated from 30**
 251 **samples of the Swiss DEM (glaciers and areas outside of proglacial areas + 200 m buffer**
 252 **excluded) after Loye et al. (2009, see text for details). The ranges where PDFs intersect**
 253 **are denoted T1 (flood plain ↔ footslopes), T2 (footslopes ↔ steep slopes) and T3 (steep**
 254 **slopes ↔ rock walls). Boxplots show the distribution of corresponding means. B: The**
 255 **intersections of the empirical slope distributions of four landform types of the**
 256 **geomorphological map of Val d’Hérens (Lambiel et al., 2016) are fairly consistent with**
 257 **the ranges T1-T3 indicated in (A). See text for details.**
 258

259 In order to assess the uncertainty of the intersection values due to sampling and iterative PDF
 260 decomposition, we repeated the PDF 30 times. We selected $k=4$ as the user-specified number
 261 of single PDFs, assuming (intuitively) that the following landform types were most
 262 representative for proglacial systems: (a) rock walls, (b) steep slopes such as scree and lateral
 263 moraines, (c) alluvial or debris cones, and (d) floodplains. We assume that these landform
 264 types have markedly different PDFs of slope, and set the following initial means, μ , and
 265 standard deviations, σ , for the iterative normalmixEM algorithm, based on preliminary
 266 analyses of proglacial systems that we are especially familiar with, i.e. Ödenwinkelkees:
 267 Carrivick et al. (2013, 2015), and Kaunertal: Heckmann et al. (2016b) as (a) $\mu=45^\circ$, $\sigma=3$; (b)
 268 $\mu=30^\circ$, $\sigma=6$; (c) $\mu=15^\circ$, $\sigma=7$; (d) $\mu=5^\circ$, $\sigma=12$. Moreover, $k=4$ is consistent with Loye et al.
 269 (2009).

270

271 **2.4 Regional relationships of proglacial hypsometry and slope**

272 One way analysis of variance (ANOVA) was used to analyse relationships between slope
 273 threshold (between hillslope-dominated and fluvially-dominated land, derived from slope-
 274 area analysis) with the categorical variables of hypsometric index and lithology. Hypsometric
 275 index was also employed as a quantitative variable to compare it in the same manner to
 276 lithology. Categories of lithology with less than 10 samples in them (sandstone, amphibolite,
 277 carbonates, meat-sediment group, marble, tonalite, sand, claystone) were excluded from the
 278 analysis for being not statistically significant. A test for equal variances was performed to
 279 identify 95% confidence intervals for the samples within each category. For each of these
 280 three relationships statistical groups were identified using Fischer's individual error rate.

281
 282 Our proglacial system outlines and distributed elevation and meltwater influence are made
 283 freely available (Carrivick, 2018). The outlines are a shapefile in UTM zone 33N projection
 284 and with attributes of drainage basin, HI and percent meltwater influence per system.
 285 Distributed elevation enables slope and hence landform classes to be computed quickly as
 286 described above in this paper. The meltwater influence grid has been extracted/clipped to
 287 proglacial system extent but was computed using a regional DEM. Note that contributing area
 288 also requires the regional DEM to be analysed.

289

290 **3. RESULTS**

291 In total we analysed 2812 proglacial systems (Austria: 23 %, Switzerland: 77 %) with a
 292 combined area of 933.5 km² (Table 1). These proglacial systems span a wide geographical
 293 area, several climatic and geological regions and a large elevation range. They have
 294 hypsometry that is predominantly equidimensional; i.e. a near-equal distribution of area at all
 295 elevations (e.g. in the Po, Rhine and Rhone drainage basins), whilst more than half of the
 296 proglacial systems within the Drava, Venetian Coast and Danube drainage basins are very
 297 bottom heavy, i.e. with much more area situated at lower elevations (Table 1).

298

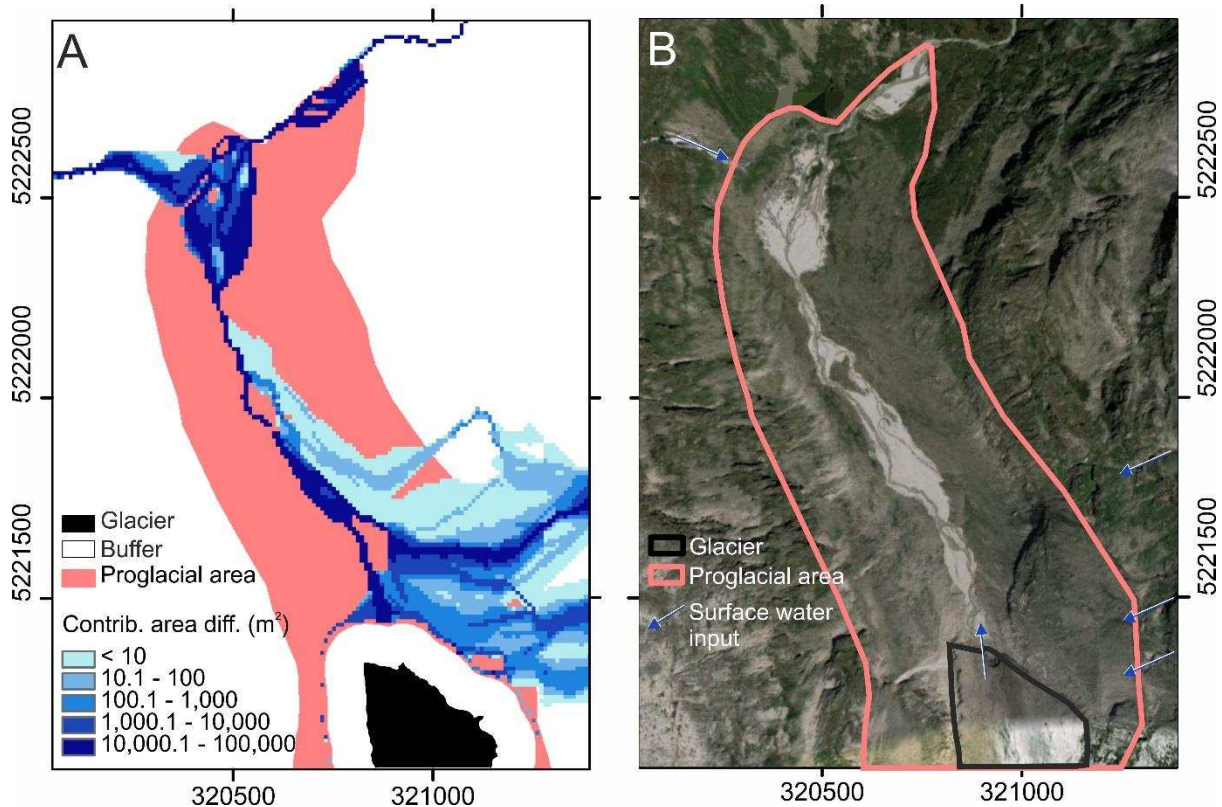
	Inn	Drava	V.Coast	Po	Rhine	Rhone	Danube
Number of proglacial systems	652	117	12	317	794	906	14
Area sum (km ²)	307.6	78.8	6.3	78.3	200.2	255.9	6.4
Elevation min. (m.asl)		1726	2209	1798			1902

Elevation max. (m.asl)	3974	3696	3357	3989	4040	4380	3276
Elevation mean (m.asl)	2679	2659	2709	2763	2581	2854	2411
Very top heavy (%)	0	0	0	0	<1	<1	0
Top heavy (%)	0	0	0	0	0	<1	0
Equidimensional (%)	49	25	42	96	96	94	36
Bottom heavy (%)	10	17	8	4	3	6	7
Very bottom heavy (%)	41	58	58	0	1	<1	57
Mean meltwater spatial influence (%)	40	48	46	16	29	29	47

Table 1. Selected statistics on the number, size and elevation distribution of 2812 proglacial systems across central Europe

3.1 Definition of spatial importance of glacial meltwater

Our spatially-distributed estimate of glacial meltwater influence agrees very well with reality, for example as shown in [figure 4](#) for the Ödenwinkelkees catchment (Carrivick et al., 2013, 2015), where glacier-fed, glacier-influenced and groundwater streams create a distinguishable patchwork of (well-studied) streams and rivers (Dickson et al., 2012; Brown et al., 2015).



308

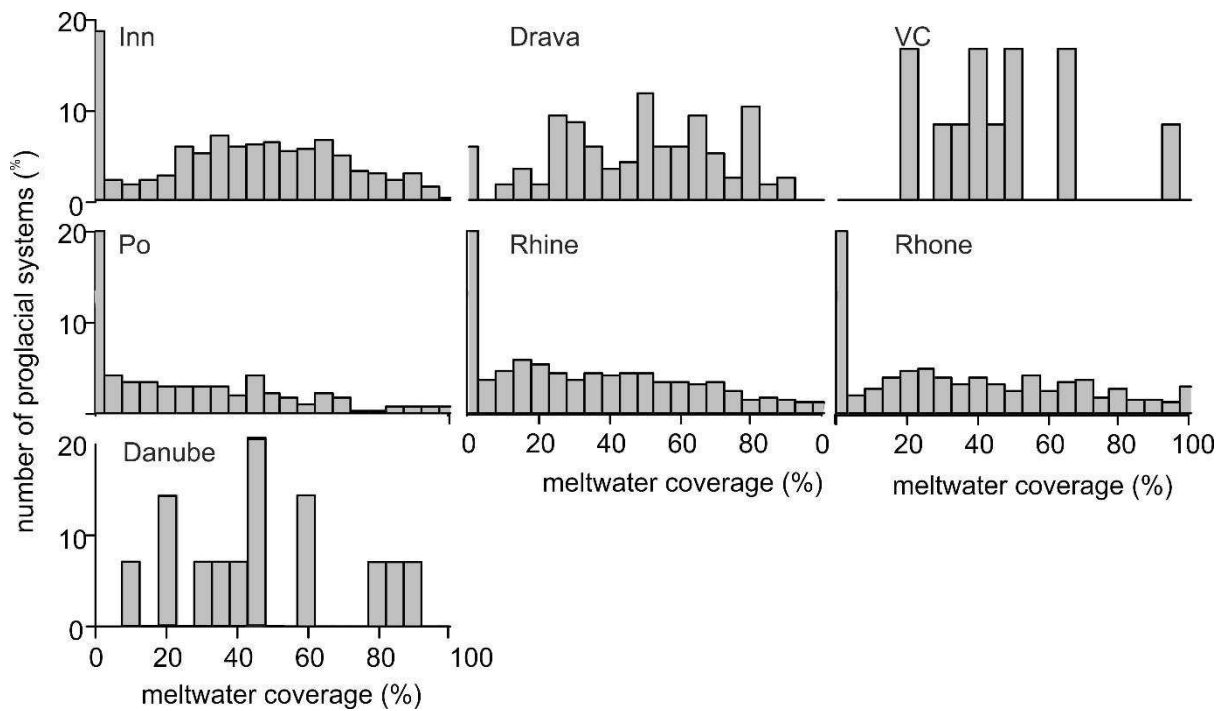
309

310 **Figure 4. Visual comparison of our contributing area-derived estimate of the spatial**
 311 **coverage and importance of glacier meltwater (A), versus reality (B), as for the**
 312 **Ödenwinkelkees catchment in central Austria, where surface water inputs are from**
 313 **Dickson et al. (2012) and Brown et al. (2015).**

314

315 Across all of the central European Alps proglacial systems the mean proportional area of
 316 proglacial systems that is probably affected by glacial meltwater is 37 %. However, there is a
 317 very wide dispersion to this data (Fig. 5) and we found no relationship between proglacial
 318 area size and percentage meltwater influence. Excluding the numerous examples of proglacial
 319 systems that apparently have no glacial meltwater influence, most obviously due to complete
 320 disappearance of glaciers from these catchments, there is a very large inter-quartile range
 321 (IQR) for proglacial systems within the seven drainage basins; specifically from and IQR of
 322 19 % (Po) to 55 % (Rhône). The meltwater coverage histogram in Figure 5 for the Inn
 323 drainage basin is normally distributed (excluding zeros), whereas those for the Po, Rhine,
 324 Rhône are skewed towards lower meltwater coverages, with modal values of ~ 5, 15 and 25
 325 %, respectively. The Drava, Venetian Coast and Danube basins have too few proglacial
 326 systems for a normality test to be significant. There are a few examples in both countries
 327 where virtually the entire area of a proglacial system is probably affected by glacial
 328 meltwater.

329

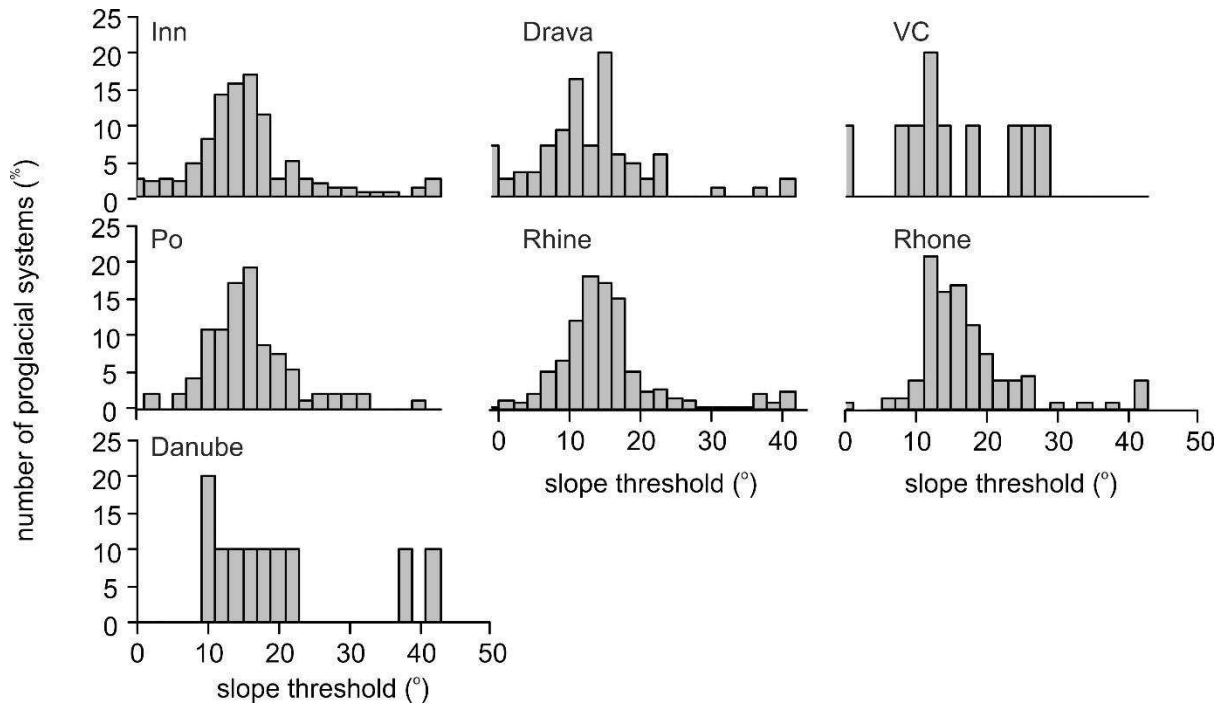


330

331 **Figure 5. Histograms of meltwater coverage (% of total proglacial system area) for each**
 332 **major drainage basin with headwaters in the central European Alps.**
 333

334 3.2 Geomorphological functioning: hillslope versus fluvial processes

335 The slope threshold determined from our slope-area analysis for separating fluvially-
 336 dominated and hillslope-dominated (mostly gravitational processes) grid cells for each
 337 proglacial system had a mean of 27° across the central European Alps. There is no
 338 statistically significant difference between the mean slope threshold values for each drainage
 339 basin (Table 2) at the 5 % significance level. Slope threshold value histograms for proglacial
 340 systems within each of the seven major drainage basins are almost normally-distributed, with
 341 the mean and median values very similar (Table 2), although the Venetian Coast and Danube
 342 datasets that are too small in number (samples) for any significant distribution to be detected
 343 (Fig. 6; Table 2).
 344



345

346

347

348

Figure 6. Histograms of the slope threshold discriminating between fluvial and hillslope-dominated grid cells for proglacial systems in the central European Alps.

	Inn	Drava	V.Coast	Po	Rhine	Rhone	Danube
Proglacial systems with identifiable slope threshold (n)	422	86	10	92	300	129	10
Mean	26	24	26	27	27	28	30
Std. dev.	18	18	18	14	18	17	24
Lower quartile	16	13	17	19	18	22	17
Median	25	22	24	27	26	27	27
Upper quartile	32	30	42	32	32	34	35

349

350

351

Table 2. Selected descriptive statistics of the slope threshold (degrees) for discriminating between hillslope-dominated and fluvially-dominated terrain

352

353

354

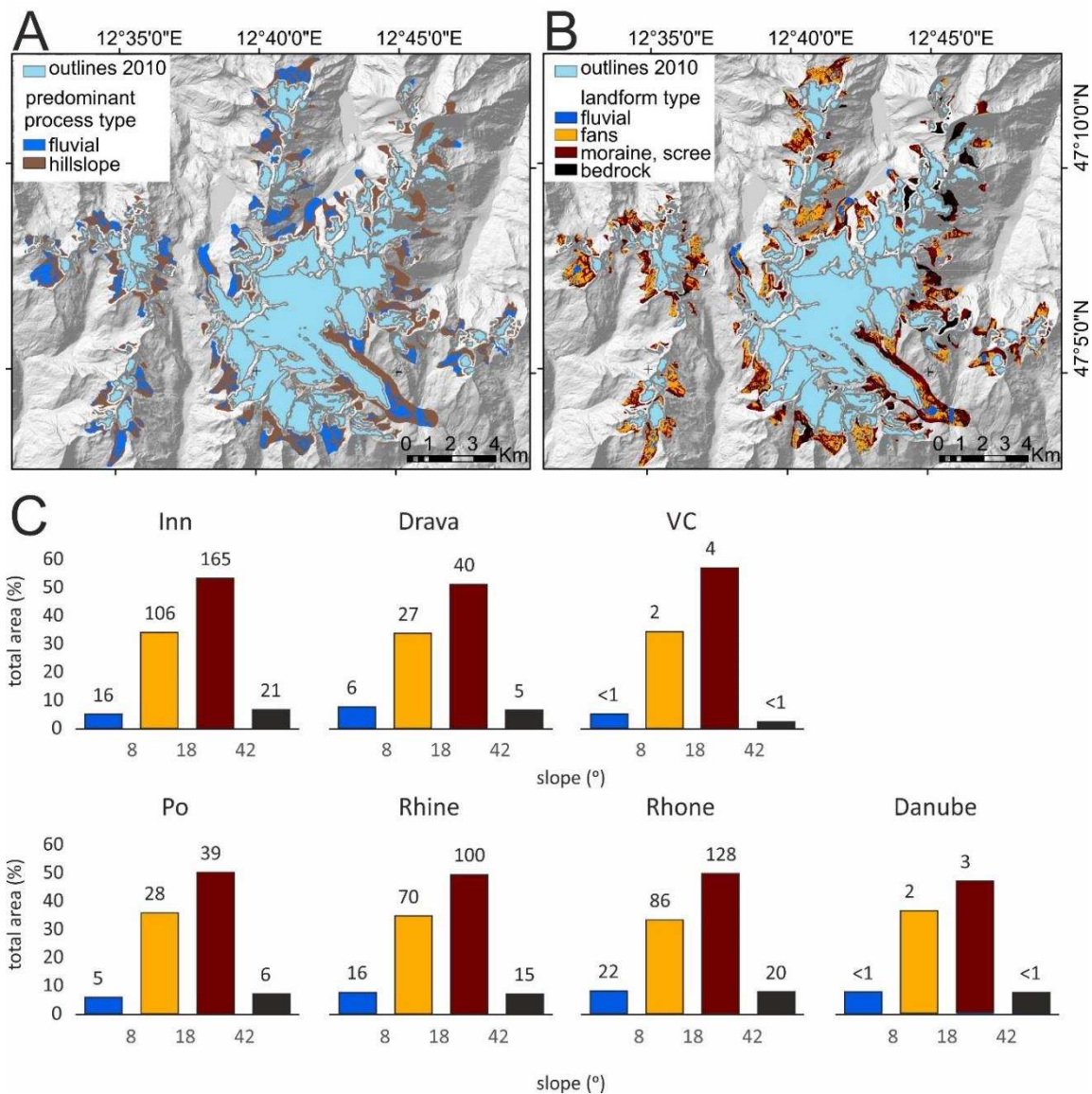
355

356

357

Analysing the slope threshold for each proglacial zone permitted calculation of the area of each proglacial zone that is predominantly affected by fluvial or by hillslope activity. Overall, 35 % of proglacial systems across the central European Alps have > 90 % of their area dominated by hillslope activity and just < 10 % of their area dominated by fluvial activity. There is wide dispersion in this data and we found no difference in the histograms of the percentage area coverage of hillslope activity between major drainage basins. [Figure 7A](#) is an

358 example of mapping out grid cells per proglacial zone coloured by whether their slope is
 359 above or below the slope threshold for that proglacial zone. This map hints at the similar total
 360 spatial coverage of each of the two major process domains. Notwithstanding that many
 361 individual systems are hillslope activity-dominated, as mentioned above. the total area that is
 362 predominantly controlled by fluvial processes is $\sim 472 \text{ km}^2$ and the total area corresponding
 363 to dominant hillslope processes is $\sim 453 \text{ km}^2$; i.e. in terms of total proglacial system land area
 364 across the central European Alps there is a 50/50 split between fluvial and hillslope
 365 dominance.

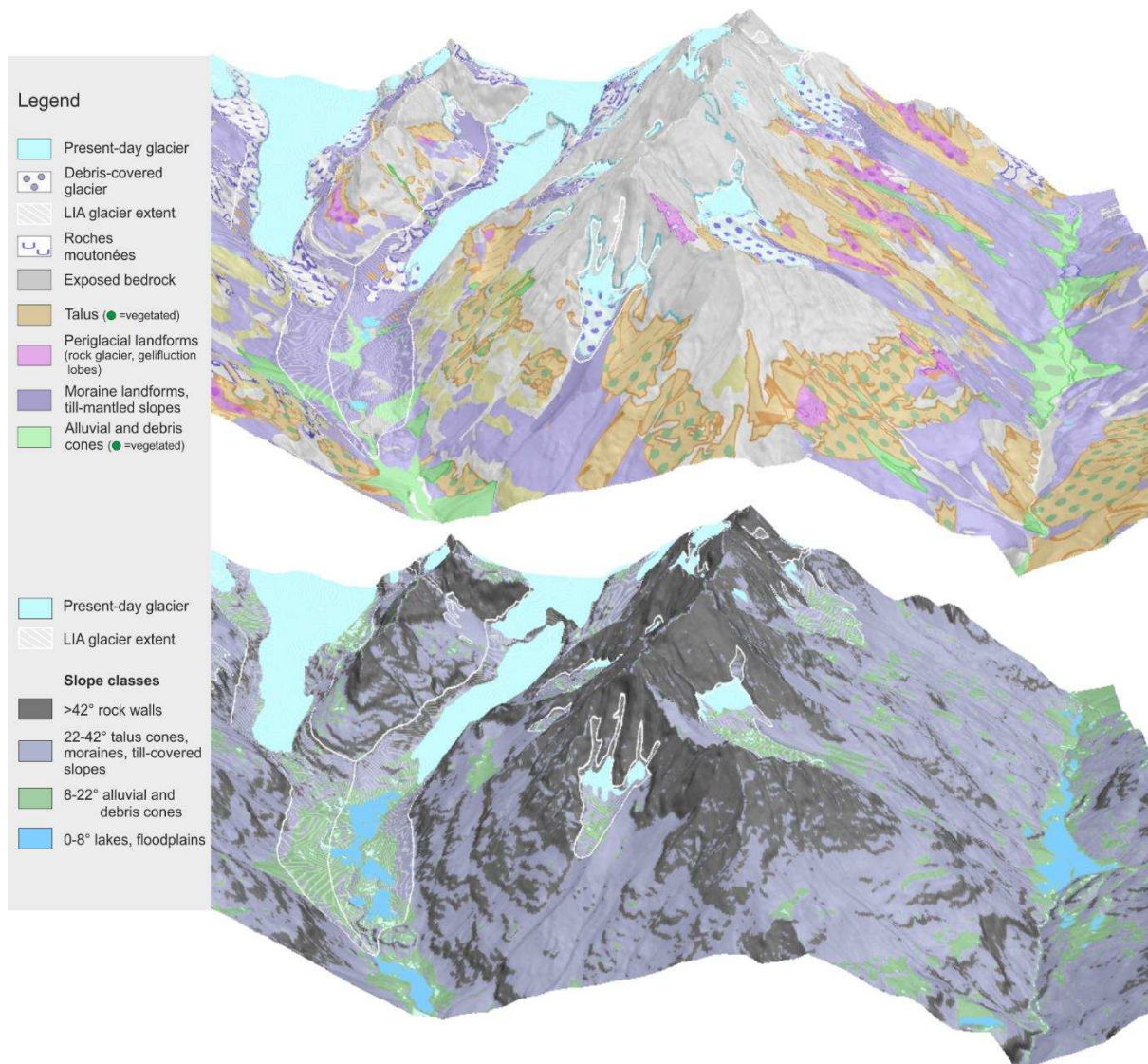


366
 367 **Figure 7. Results of the slope-contributing area scatterplot analysis to suggest a slope**
 368 **threshold to separate predominant major geomorphological process domains (A), and**
 369 **of PDF analysis on slope values within proglacial systems (A), both displayed in map**
 370 **form for the Grossglockner area of Austria. Relative spatial coverage of each major**
 371 **landform type for each major drainage basin with numbers on top of bars giving**
 372 **absolute area (km²) (C).**

373

374

3.3 Geomorphological composition



375

376

377

378

379

380

381

382

Figure 8. Three-dimensional perspective visualisation of the Val d'Hérens, Switzerland. The upper part shows a generalised version of a geomorphological map published by Lambiel et al. (2016). The lower panel presents our slope-based classification; the thresholds separating the slope categories were derived from the distribution of slope of the Swiss DEM10 (except present-day glaciers) following Løye et al. (2009), leading to a first-order classification of proglacial systems geomorphology.

383

384

385

386

387

Our slope-based geomorphological classification agrees well visually with reality as measured either from our own experience (Ödenwinkelkees: Carrivick et al., 2013, 2015; Kaunertal: Heckmann et al., 2016) or from published geomorphological maps such as that by Lambiel et al. (2016) for the Val d'Herens (Fig. 8). We attempted a quantitative measurement of the 'goodness of agreement' in these figure 8 maps but that was hampered by differences

388 in the mapping, such as Lambiel et al. (2016) did not map rock walls. [Figure 7B](#) maps out
389 grid cells coloured by which landform class they belong to, as discriminated by the PDF
390 analysis. This is essentially a rudimentary automated geomorphological mapping with
391 advantages over expert judgement-driven mapping of being fast, repeatable and easily
392 applied across multiple sites and large (mountain range) scales simultaneously. The
393 proportions of the combined proglacial system area belonging to each landform class is
394 remarkably similar between each of the seven major drainage basins, with > 5 % fluvial, ~35
395 % fans, ~50 % moraine ridges and talus/scree, and ~ 10 % bedrock ([Fig. 7C](#)).

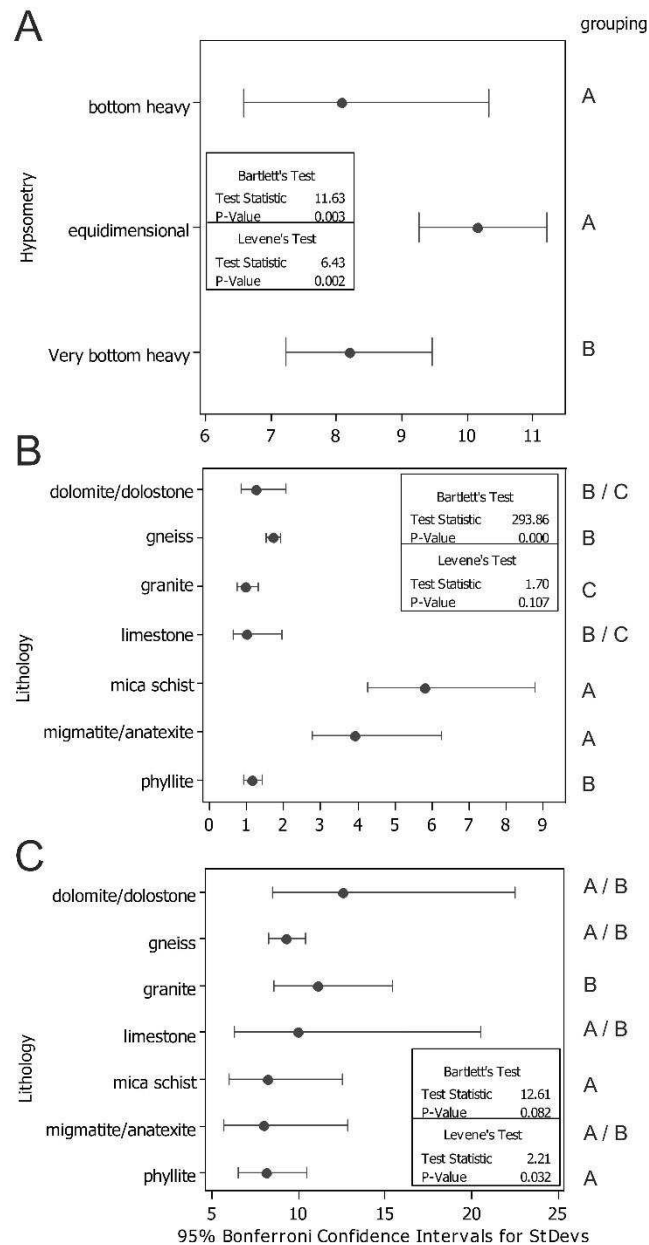
396

397 **3.4 Regional associations and patterns**

398 No trend was detected in the slope threshold with east-west or with north-south location
399 across the central European Alps so it is apparently not associated with regional variations
400 such as climate. However, the relationship between slope threshold and hypsometric index
401 identifies two statistically different groups. Specifically, proglacial systems with
402 ‘equidimensional’ hypsometry have a slope threshold of mean 22.9 degrees that is
403 statistically different to the mean of 25.3 degrees of proglacial systems with ‘very bottom
404 heavy’ (most area situated at lower elevation) hypsometry. Proglacial systems with bottom
405 heavy hypsometry have a mean slope threshold of 26.4 degrees but the dispersion of the data
406 is sufficiently great for it to belong to both groups, p-value 0.002 ([Fig. 9A](#)).

407

408 Three statistically different groups exist between hypsometric index and lithology. Proglacial
409 systems underlain by mica schist, magmatite and marlstone all belong to one group in terms
410 of their slope threshold, gneiss and phyllite belong to a second group, and granite belongs to a
411 third group. We note an association of these three groups with grain size, where group 1
412 rocks are fine/medium-grained, group 2 are medium/coarse-grained, and group 3 has large
413 grains. Statistically, dolomite could belong to either group 2 or 3, p value 0.107 ([Fig. 9B](#)).



414

415

416 **Figure 9. Test for equal variances and identification of statistical groupings of slope**
 417 **threshold discriminating between hillslope- and fluviially-dominated terrain within**
 418 **proglacial systems of each hypsometric class (A), of hypsometric index with lithology**
 419 **(B), and of slope threshold with lithology (C). Note varying x-scale between panels. Note**
 420 **groupings are not transferable between panels.**

421

422 Analysis of the relationship between slope threshold and lithology identified two groups; one
 423 comprising mica schist and phyllite, which are both very well bedded/foliated metamorphic
 424 rocks, and one comprising granite, which is a massive igneous rock. Dolomite, limestone,
 425 migmatite and gneiss could all statistically belong to either group and are either crystalline
 426 sedimentary or metamorphic rocks (Fig. 9C). A relationship between rock hardness and the

427 slope threshold discriminating between fluvial and hillslope processes (p-value 0.002) is
428 apparently non-linear and most likely so because phyllite and mica-schist are strongly
429 bedded/foliated and across the central European Alps tend to maintain a high angle of
430 inclination (Fig. 9C).

431

432 **4. DISCUSSION**

433 On the basis of our definition of proglacial systems being most simply represented by land
434 area between LIA and contemporary glacier margins, we discriminate parts of alpine
435 landscapes that have undergone rapid short term evolution. On the basis of a series of
436 geometric measurements alone it was extremely difficult to identify groupings or patterns in
437 topographic metrics of the proglacial systems of the central European Alps. That was a
438 surprise given that proglacial systems are conventionally assumed to be created or at least
439 primarily conditioned by glaciation (Church and Ryder, 1972) and that those glacial
440 processes are dependent on climate-topography interactions (Raper and Braithwaite, 2009),
441 which vary systematically with location across the European Alps. Nonetheless we were able
442 to spatially characterise geomorphological functioning, landform type, meltwater influence
443 and estimate rates of landscape evolution, all of which are precursors to making informed
444 land and water management across Europe in terms of natural hazards, natural resources,
445 habitat and water quality and ecosystem services, for example.

446

447 **4.1 Coverage of major geomorphological process domains**

448 We have used a slope threshold value of between 24° and 30° (mean 27°) to quickly
449 discriminate geomorphological functioning; hillslope-dominated (mostly gravitational
450 processes) land surfaces that are steeper than that threshold value, versus fluvially-dominated
451 land surfaces that are shallower than that threshold. Throughout the central European Alps
452 and within most of the proglacial systems that we have analysed it is hillslope-dominated
453 land that covers the greater proportion of proglacial systems. This terrain we interpret to
454 represent gravity-driven falls and slumps rather than fluvially-influenced slides and flows. As
455 an aside we emphasise our use of the word ‘dominated’; fluvial processes will occur on
456 slopes steeper than our threshold and hillslope-gravity processes will occur on slopes
457 shallower than our threshold. A predominance of hillslope-dominated land surface(s) implies
458 that greater proportions of proglacial systems are sediment sources and temporary storages,
459 as represented by bedrock cliff falls, debris slumps on talus/scree slopes for example. It
460 follows that the minority of land surface within proglacial systems is fluvially-dominated and

461 therefore comprises major sediment pathways and exports. Our recognition of proglacial
462 systems being hillslope-dominated suggests that that there is an abundant sediment supply, as
463 Maisch et al. (1999) and most recently Schoch et al. (2018) have quantified. Furthermore,
464 these measurements strongly suggest that proglacial systems are most likely to be sediment
465 transport-limited, which has implications for statistical or empirical modelling of sediment
466 transfer (e.g. Bennett et al., 2014; Capt et al., 2016).

467

468 **4.2 Landforms**

469 Our separation of slope classes identified three statistical boundaries and thus four landform
470 groups. For slopes above the 42° boundary, bedrock is interpreted as a source / generation
471 zone of sediment and also as a landcover that generates instantaneous runoff from rainfall.
472 Talus/scree is the predominant geomorphological entity occupying 26° to 42° slopes and this
473 is a temporary sediment store, initially produced as a paraglacial response soon after
474 deglaciation and destabilisation of surrounding slopes, but then reactivated with additional
475 rockfall (e.g. Kellerer-Pirklbauer et al., 2012), debris flows, intense rainfall, permafrost
476 degradation or undercutting by rivers, for example. Another typical landform contained in
477 this slope interval are steep lateral and terminal moraines (although those can maintain slopes
478 much steeper than 42°, c.f. Lukas et al. 2012). Therefore a slope of 26° is interpreted as a
479 good estimate in general of a slope threshold between sediment entrainment zones or scour as
480 represented in gullies, many of which are fan-head. Debris fall deposits, debris flow deposits
481 and alluvial fans occupy slopes between 26° and 8° and from our widespread field campaigns
482 are apparently zones almost entirely of deposition with volumetrically minor reactivation.
483 Thus they are at least in the short term a sediment sink. Indeed it is coalescing fans that
484 commonly intercalate with valley fill (braided river and floodplain deposits) to submerge
485 many alpine valley floors, as we ourselves have observed in the Ödenwinkelkees, Kaunertal
486 and as Lambiel et al. (2016) map for the Val d'Hérens (Fig. 8).

487

488 **4.3 Water, sediment and solute (WSS) fluxes**

489 WSS sources in proglacial systems comprise glaciers, snow packs, eroding gullies, re-
490 activated fans and river banks. The extremely wide dispersion of values of spatial meltwater
491 influence that we have quantified demonstrates that assumptions of the predominance of
492 glacially-sourced meltwater and fluvially-transported sediment and solute in defining
493 proglacial system character and functioning are rather over-simplifying reality. At least
494 spatially that simplification is apparent, although temporally it is well known that episodic

495 floods can do a lot of geomorphological work (e.g. Warburton, 1990; Staines et al., 2015)
496 despite being restricted to a small proportion of a proglacial system area.

497

498 Our analysis has identified likely glacial meltwater pathways and offers an estimate of the
499 spatial coverage, or importance of this meltwater. That spatial importance could be taken as a
500 first-order indication of the sensitivity of a proglacial system to a (future) change in glacial
501 ice meltwater contribution. Such meltwater sensitivity analyses have recently been performed
502 globally, i.e. per major drainage basin, by Huss and Hock (2018) but they report considerable
503 sub-basin (i.e. inter-catchment) variability. In this study we have demonstrated a quick
504 method for quantifying the spatial coverage, or spatial influence, of glacial meltwater and we
505 have shown that varies enormously between proglacial systems within a region and is
506 independent of any recent change in glacier size. We contend that steeper narrower valleys
507 tend to transmit water and sediment beyond a proglacial system, whereas wider shallower
508 valleys tend to permit sediment deposition and progressive aggradation as glaciers diminish.
509 Such spatial analysis and such system sensitivity analysis are both important for
510 understanding intra- and inter-catchment river channel stability, spatio-temporal water
511 temperature regime (Carrivick et al., 2012) and habitat suitability for a wide range of aquatic
512 and riparian organisms (Milner et al., 2017; Fell et al., 2017).

513

514 **4.4 Landscape evolution**

515 A slope threshold of $\sim 10^\circ$ was proposed by Palacios et al. (2011) to delimit between debris
516 flow and fluvially-dominated terrain in Meteor Crater. Their value is very much lower than
517 ours for alpine landscapes due to lithology. In the relatively soft (mostly sandstone)
518 sediments of Meteor Crater, debris flows cut gullies and fill in troughs, and fluvial processes
519 deliver more sediment and incise the fine-grained material, so that there is a feedback
520 between these debris flow and fluvial processes and both are necessary for landscape
521 evolution. On harder lithologies, with higher tensile strength, such as are typical across the
522 European central Alps, the work of Sklar and Dietrich (2001, 2006) has shown that debris
523 flows will be the primary mechanism by which bedrock incision occurs on steep slopes after
524 deglaciation. This, they report, means that grain size is a key control on bedrock incision and
525 geomorphological work achieved, which seems to be reinforced by our identification of a link
526 between our slope threshold value and our groupings of lithology (Fig. 9). Indeed, grain size
527 control (and rock hardness and sediment supply) has been used to explain scatter that is
528 common in the tail, the fluvial end, of slope-area power law plots (e.g. our eqn. 1). Landform

529 and landscape evolution is very dependent on sediment supply and there is a critical
530 threshold, which is yet to be ascertained for proglacial systems, whereby too much sediment
531 supply produces land surfaces becoming ‘drowned’, and whereby too little retards abrasion
532 and thus incision. Across the central European Alps Maisch et al. (1999) remarked that
533 sedimentary and mixed sedimentary-rocky glacier beds dominate and so in general sediment
534 supply should be high and valley-fill sediment should persist where topography permits.
535 Valley infill sediments can be detected automatically using low-angle slope filters and as this
536 study has shown major depositional landforms such as alluvial and debris fans can also be
537 discriminated with slope-based analyses.

538

539 **4.5 Implications for estimating regional proglacial erosion rates**

540 Our maps of meltwater influence, of landforms and of major earth surface processes each
541 offer important information for water and land management, such as characterising
542 (evolving) sediment (and solute) sources, pathways and sinks, hillslope and channel stability
543 and thus habitat character and quality. Together these datasets are several of the components
544 necessary to estimate spatially-distributed (inter-catchment) proglacial geomorphology,
545 which can vary markedly between catchments (e.g. Carrivick and Rushmer, 2009), and erosion
546 rates. However, additional data is required on representative erosion rates for different
547 landform classes and as Carrivick and Heckmann (2017; their figure 10) have shown there
548 are very few direct measurements and a very wide range of values, for each landform class.
549 The recent study by Delaney et al. (2017) emphasises problems within a catchment of levels
550 of detection, over-printing (erosion at a point subsequently obscured by deposition), and of
551 converting volume to mass loss (e.g. with debris-covered ice-cored moraine), even with well-
552 constrained annual DEMs spanning > 25 years.

553

554 To estimate a regional erosion rate, there are problems with applying a relationship from a
555 single proglacial system to all systems because there are many controls on erosion rate other
556 than proglacial area, such as connectivity, area impacted by meltwater etc. Nonetheless, if we
557 assume that the > 25 year data reported in Delaney et al.’s (2017) figure 3 is representative of
558 proglacial systems (spatially and contemporaneously) across the European Alps a polynomial
559 relationship ($r^2 = 0.96$) can be created between volume change and proglacial area (km^2).
560 Then it is possible to estimate a contemporary total volume loss of $44,003,800 \text{ m}^3\text{a}^{-1}$ for all
561 central European proglacial systems combined, which equates to a mean of $0.3 \text{ mm}\cdot\text{a}^{-1}$
562 contemporary surface lowering. These mean values are a snapshot and an estimate only. They

563 hide the dominant contributions of fewer larger proglacial systems, although 99 % of all our
564 estimates were $< 16 \text{ mm.a}^{-1}$. The mean values are greater than the postglacial erosion rates
565 (surface lowering equiv. 0.15 mm.a^{-1}) calculated by Campbell and Church (2003) and
566 Hoffman et al. (2013) for the Coast Mountains of British Columbia, but an order of
567 magnitude less than suggested by single site analyses within the European Alps of
568 geomorphological evidence (e.g. 30 mm.a^{-1} to 90 mm.a^{-1} Curry et al., 2006) and of multi-
569 temporal proglacial DEMs (e.g. 34 mm.a^{-1} : Carrivick et al., 2013). They are several orders of
570 magnitude greater than estimates derived from sedimentation within proglacial lakes or
571 reservoirs (as summarised in Carrivick and Heckmann, 2017) which only capture net material
572 efflux rather than intra-catchment mobility. Nonetheless, they probably represent a good
573 estimate of regionally-averaged contemporary rates, especially given that proglacial systems
574 are rapidly expanding and adjusting to climate change through deglaciation, permafrost
575 degradation and meltwater and precipitation regime shifts.

576

577 **5. SUMMARY AND CONCLUSIONS**

578 We have presented the first quantification of the topography and geomorphological
579 composition of proglacial systems across the central European Alps, and specifically for 2812
580 sites across Austria and Switzerland. We make these system outlines and distributed
581 elevation data freely available (Carrivick, 2018). We found no association of topographic
582 metrics with location, which we supposed might represent patterns of climatic influence.
583 However, we did find statistically different groups in terms of a relationship between
584 hypsometric index and lithology, and of slope threshold with lithology. Proglacial systems
585 underlain by mica schist, magmatite and marlstone all belong to one group, gneiss and
586 phyllite belong to a second group, and granite belongs to a third group. These relationships
587 suggest that grain size is a key control not only on proglacial system topography but also on
588 the spatial patterning and relative importance of hillslope (mostly gravitational processes)
589 versus fluvial processes and thus on system status as sediment supply- or sediment transport-
590 limited.

591

592 For each proglacial system we have defined the spatial coverage of hillslope versus valley-
593 floor fluvial processes and used these to evaluate the spatial arrangement and importance of
594 likely WSS sources, pathways and sinks. Across the central European Alps the proportions of
595 the total proglacial system area belonging to each landform class is remarkably similar, with
596 $> 5 \%$ fluvial, $\sim 35 \%$ fans, $\sim 50 \%$ moraine ridges and talus/scree, and $\sim 10 \%$ bedrock.

597 Identification of the spatial occurrence and importance of these landform classes is very
598 helpful for assessing future earth surface processes and landscape stability, such as via
599 sediment yield and denudation rate calculations, for example, as well as for habitat
600 development because these landforms are the local platform upon which mass movements,
601 soil development and biological activity all react to climate change and human-influenced
602 changes. The spatial association, stability and preservation of these landforms changes
603 perhaps most recognisably in terms of surface connectivity, and as micro-topography and
604 micro-climates permit (e.g. Eichel et al., 2016). As a first-order estimate of the contemporary
605 geomorphological activity and thus landscape evolution represented by the spatial coverage
606 of these landform classes, we propose a total volume loss from all these proglacial systems
607 equivalent to a mean of 0.3 m.a^{-1} surface lowering.

608

609 In conclusion, proglacial systems have become exposed following retreat of glaciers from
610 their LIA margin positions, and have subsequently developed transitioning from glacier-
611 dominated processes to paraglacial processes. Quantifying topographic and
612 geomorphological composition and functioning of proglacial systems is a first and necessary
613 step towards understanding processes driving volume and mass changes within (and exports
614 from) proglacial systems, which themselves are essential for land (stability) and water
615 (quantity and quality) management, hazard analyses and definition of alpine ecosystem
616 services.

617

618 We have presented the first regional scale assessment of proglacial system geomorphological
619 composition and functioning and we have done this in a rapid and efficient manner. Our
620 quantitative analysis can be developed towards providing assessments of alpine landscape
621 sensitivity to climate change, most simply start with spatial analyses considering that the
622 most unstable parts of the landscape are where slope is high and soft sediment is present, and
623 the most stable parts are where slopes are low and soft sediment is absent. Future work on
624 landform evolution within proglacial systems could exploit our datasets for determining
625 sediment distribution and sediment supply across proglacial systems (as opposed to from a
626 glacier), and across alpine landscapes, via multivariate geostatistical modelling (Schoch et al.,
627 2018) and via calculation of spatially-distributed (intra-catchment) sediment budget ratios
628 from repeat DEMs (Heckmann and Vericat, 2018), respectively.

629

630

631 **REFERENCES**

- 632 Asch, K., 2003. The 1:5 Million International Geological Map of Europe and Adjacent Areas:
633 Development and Implementation of a GIS-enabled Concept; *Geologisches Jahrbuch*; SA 3, BGR,
634 Hannover (ed.); Schweitzerbart (Stuttgart), 190 p., 45 fig., 46 tab.
- 635 Ballantyne, C.K., 2002. Paraglacial geomorphology. *Quaternary Science Reviews* 21:1935-2017.
- 636 Benaglia, T., Chauveau, D., Hunter, D.R., Young, D., 2009. mixtools: An R Package for Analyzing
637 Finite Mixture Models. *Journal of Statistical Software* 32, 1-29.
- 638 Bennett, G.L., Molnar, P., McArdeell, B.W., Burlando, P., 2014. A probabilistic sediment cascade
639 model of sediment transfer in the Illgraben. *Water Resources Research* 50:1225-1244.
- 640 Beylich, A.A., Laute, K., Storms, J.E., 2017. Contemporary suspended sediment dynamics within two
641 partly glacierized mountain drainage basins in western Norway (Erdalen and Bødalen, inner
642 Nordfjord). *Geomorphology* 287:126-143.
- 643 Brown, L.E., Dickson, N.E., Carrivick, J.L. Fuereder, L., 2015. Alpine river ecosystem response to
644 glacial and anthropogenic flow pulses. *Freshwater Science* 34:1201-1215.
- 645 Capt, M., Bosson, J.B., Fischer, M., Micheletti, N. and Lambiel, C., 2016. Decadal evolution of a very
646 small heavily debris-covered glacier in an Alpine permafrost environment. *Journal of Glaciology*
647 62:535-551.
- 648 Carrivick, J.L., 2018. Contemporary central European proglacial areas. <dataset DOI>
- 649 Carrivick J.L., Heckmann, T., Fischer, M., Davies, B., (accepted) An inventory of proglacial systems
650 in Austria, Switzerland and across Patagonia. In: Heckmann T, Morche D (Eds) *Geomorphology of*
651 *Proglacial Systems. Landform and Sediment Dynamics in Recently Deglaciaded Alpine Landscapes.*
652 Springer International Publishing
- 653 Carrivick, J.L., Heckmann, T., 2017. Short-term geomorphological evolution of proglacial systems.
654 *Geomorphology* 287:3-28.
- 655 Carrivick, J.L., Rushmer, E.L., 2009. Inter-and intra-catchment variations in proglacial
656 geomorphology: an example from Franz Josef Glacier and Fox Glacier, New Zealand. *Arctic,*
657 *Antarctic, and Alpine Research* 41:18-36.
- 658 Carrivick, J.L., Berry, K., Geilhausen, M., James, W.H., Williams, C., Brown, L.E., Rippin, D.M.,
659 Carver, S.J., 2015. Decadal-scale changes of the Ödenwinkelkees, central Austria, suggest increasing
660 control of topography and evolution towards steady state. *Geografiska Annaler: Series A, Physical*
661 *Geography* 97:543-562.
- 662 Carrivick, J.L., Geilhausen, M., Warburton, J., Dickson, N.E., Carver, S.J., Evans, A.J., Brown, L.E.,
663 2013. Contemporary geomorphological activity throughout the proglacial area of an alpine catchment.
664 *Geomorphology* 188:83-95.
- 665 Carrivick, J.L., Brown, L.E., Hannah, D.M., Turner, A.G., 2012. Numerical modelling of spatio-
666 temporal thermal heterogeneity in a complex river system. *Journal of Hydrology* 414:491-502.
- 667 Campbell, D., Church, M., 2003. Reconnaissance sediment budgets for Lynn Valley, British
668 Columbia: Holocene and contemporary time scales. *Canadian Journal of Earth Sciences* 40:701-713.
- 669 Church, M., Ryder, J.M., 1972. Paraglacial sedimentation: a consideration of fluvial processes
670 conditioned by glaciation. *Geological Society of America Bulletin* 83:3059-3072.
- 671 Curry, A.M., Cleasby, V., Zukowskyj, P., 2006. Paraglacial response of steep, sediment-mantled
672 slopes to post-'Little Ice Age' glacier recession in the central Swiss Alps. *Journal of Quaternary*
673 *Science* 21:211-225.
- 674 Daten Österreichs. 2016. Digitales Geländemodell (DGM) Österreich.
675 <https://www.data.gv.at/katalog/dataset/b5de6975-417b-4320-afdb-eb2a9e2a1dbf>. Last visited March,
676 2016.

- 677 Delaney, I., Bauder, A., Huss, M., Weidmann, Y., 2018. Proglacial erosion rates and processes in a
678 glacierized catchment in the Swiss Alps. *Earth Surface Processes and Landforms* 43:765-778.
- 679 Dickson, N.E., Carrivick, J.L., Brown, L.E., 2012. Flow regulation alters alpine river thermal regimes.
680 *Journal of Hydrology* 464:505-516.
- 681 EEA., 2009. Regional climate change and adaptation — The Alps facing the challenge of changing
682 water resources. <https://www.eea.europa.eu/publications/alps-climate-change-and-adaptation-2009>
683 [last visited February 2018](https://www.eea.europa.eu/publications/alps-climate-change-and-adaptation-2009).
- 684 Eichel, J., Corenblit, D., Dikau, R., 2016. Conditions for feedbacks between geomorphic and
685 vegetation dynamics on lateral moraine slopes: a biogeomorphic feedback window. *Earth Surface*
686 *Processes and Landforms* 41:406-419.
- 687 Fell, S.C., Carrivick, J.L., Brown, L.E., 2017. The Multitrophic Effects of Climate Change and
688 Glacier Retreat in Mountain Rivers. *BioScience* 67:897-911.
- 689 Fischer, M., Huss, M., Barboux, C., Hoelzle, M., 2014. The new Swiss Glacier Inventory SGI2010:
690 relevance of using high-resolution source data in areas dominated by very small glaciers. *Arctic,*
691 *Antarctic, and Alpine Research* 46:933-945.
- 692 Fischer, A., Seiser, B., Stocker-Waldhuber, M., Abermann, J., 2015a. The Austrian Glacier Inventory
693 GI 3, 2006, in ArcGIS (shapefile) format. doi: 10.1594/PANGAEA.844985
- 694 Fischer, M., Huss, M., Hoelzle, M., 2015b. Surface elevation and mass changes of all Swiss glaciers
695 1980–2010. *The Cryosphere* 9:525-540.
- 696 Glaziologie Österreich (2016). Österreichische Gletscherinventare (GI).
697 <http://www.glaziologie.at/gletscherinventar.html> Last visited March, 2016.
- 698 Groß, G., Patzelt, G., 2015. The Austrian Glacier Inventory for the Little Ice Age Maximum (GI LIA)
699 in ArcGIS (shapefile) format. doi: 10.1594/PANGAEA.844987
- 700 Heckmann, T., Morche, D., (Eds) (in press) *Geomorphology of Proglacial Systems; Landform and*
701 *Sediment Dynamics in Recently Deglaciated Alpine Landscapes*. Springer International Publishing
- 702 Heckmann, T., Vericat, D., 2018. Computing spatially distributed sediment delivery ratios: Inferring
703 functional sediment connectivity from repeat high-resolution Digital Elevation Models. *Earth Surface*
704 *Processes and Landforms* 43: 1547–1554.
- 705 Heckmann, T., McColl, S., Morche, D., 2016a. Retreating ice: research in pro-glacial areas matters.
706 *Earth Surface Processes and Landforms* 41:271-276.
- 707 Heckmann, T., Hilger, L., Vehling, L., Becht, M., 2016b. Integrating field measurements, a
708 geomorphological map and stochastic modelling to estimate the spatially distributed rockfall sediment
709 budget of the Upper Kaunertal, Austrian Central Alps. *Geomorphology* 260:16-31.
- 710 Hoffmann, T., Müller, T., Johnson, E.A., Martin, Y.E., 2013. Postglacial adjustment of steep, low-
711 order drainage basins, Canadian Rocky Mountains. *Journal of Geophysical Research: Earth Surface*
712 118:2568-2584.
- 713 Huss, M., 2011. Present and future contribution of glacier storage change to runoff from macroscale
714 drainage basins in Europe. *Water Resources Research* 47: W07511.
- 715 Huss, M., Hock, R., 2018. Global-scale hydrological response to future glacier mass loss. *Nature*
716 *Climate Change* 8:135-142.
- 717 IGME (2016). International Geological Map of Europe.
718 <http://www.bgr.de/karten/IGME5000/igme5000.htm> last visited October 2016.
- 719 Jiskoot, H., Curran, C.J., Tessler, D.L., Shenton, L.R., 2009. Changes in Clemenceau Icefield and
720 Chaba Group glaciers, Canada, related to hypsometry, tributary detachment, length–slope and area–
721 aspect relations. *Annals of Glaciology* 50:133-143.

- 722 Kellerer-Pirklbauer, A., Lieb, G.K., Avian, M., Carrivick, J.L., 2012. Climate change and rock fall
723 events in high mountain areas: Numerous and extensive rock falls in 2007 at Mittlerer Burgstall,
724 Central Austria. *Geografiska Annaler: Series A, Physical Geography* 94:59-78.
- 725 Kociuba, W., 2017. Assessment of sediment sources throughout the proglacial area of a small Arctic
726 catchment based on high-resolution digital elevation models. *Geomorphology* 287:73-89.
- 727 Lambiel, C., Maillard, B., Kummert, M., Reynard, E., 2016. Geomorphology of the Hérens valley
728 (Swiss Alps). *Journal of Maps* 12:160-172.
- 729 Lane, S.N., Bakker, M., Gabbud, C., Micheletti, N., Saugy, J.N., 2017. Sediment export, transient
730 landscape response and catchment-scale connectivity following rapid climate warming and Alpine
731 glacier recession. *Geomorphology* 277:210-227.
- 732 Litschauer, 2014. Save the alpine rivers!
733 http://www.ecrr.org/Portals/27/Events/ERRC2014/Presentations/28%20october%202014/session6/STAR_ERRC_2014.pdf last visited February 2018.
734
- 735 Loye, A., Jaboyedoff, M., Pedrazzini, A., 2009. Identification of potential rockfall source areas at a
736 regional scale using a DEM-based geomorphometric analysis. *Natural Hazards and Earth System*
737 *Sciences*, 9:1643-1653.
- 738 Lukas, S., Graf, A., Coray, S., Schlüchter, C., 2012. Genesis, stability and preservation potential of
739 large lateral moraines of Alpine valley glaciers—towards a unifying theory based on Findelengletscher,
740 Switzerland. *Quaternary Science Reviews* 38:27-48.
- 741 Maisch, M., 2000. The long-term signal of climate change in the Swiss Alps: Glacier retreat since the
742 end of the Little Ice Age and future ice decay scenarios. *Geogr. Fis. Dinam. Quat.*, 23:139-151.
- 743 Maisch, M., Haeberli, W., Hoelzle, M., Wenzel, J., 1999. Occurrence of rocky and sedimentary glacier
744 beds in the Swiss Alps as estimated from glacier-inventory data. *Annals of Glaciology* 28:231-235.
- 745 Micheletti, N., Lane, S.N., 2016. Water yield and sediment export in small, partially glaciated Alpine
746 watersheds in a warming climate. *Water Resources Research* 52:4924-4943.
- 747 Milner, A.M., Khamis, K., Battin, T.J., Brittain, J.E., Barrand, N.E., Füreder, L., Cauvy-Fraunié, S.,
748 Gíslason, G.M., Jacobsen, D., Hannah, D.M., Hodson, A.J., 2017. Glacier shrinkage driving global
749 changes in downstream systems. *Proceedings of the National Academy of Sciences* 114:9770-9778.
- 750 Palacios, M.C., Dietrich, W. E., Howard, A., 2011. [http://www.ijege.uniroma1.it/rivista/5th-
751 international-conference-on-debris-flow-hazards-mitigation-mechanics-prediction-and-
752 assessment/topic-3-debris-flow-deposits-and-fan-morphology/the-role-of-debris-flows-in-the-origin-
753 and-evolution-of-gully-systems-on-crater-walls-martian-analogs-in-meteor-crater-arizona-usa/ijege-
754 11-bs-palucis-et-alii.pdf](http://www.ijege.uniroma1.it/rivista/5th-international-conference-on-debris-flow-hazards-mitigation-mechanics-prediction-and-assessment/topic-3-debris-flow-deposits-and-fan-morphology/the-role-of-debris-flows-in-the-origin-and-evolution-of-gully-systems-on-crater-walls-martian-analogs-in-meteor-crater-arizona-usa/ijege-11-bs-palucis-et-alii.pdf)
- 755 Schoch, A., Blöthe, J.H., Hoffmann, T., Schrott, L., 2018. Multivariate geostatistical modeling of the
756 spatial sediment distribution in a large scale drainage basin, Upper Rhone, Switzerland.
757 *Geomorphology* 303:375-392.
- 758 Sklar, L. S., Dietrich, W. E., 2001. Sediment and rock strength controls on river incision into bedrock.
759 *Geology* 29: 1087-1090.
- 760 Sklar, L. S., Dietrich, W. E., 2006. The role of sediment in controlling steady-state bedrock channel
761 slope: Implications of the saltation–abrasion incision model. *Geomorphology* 82:58-83.
- 762 Staines, K.E., Carrivick, J.L., Tweed, F.S., Evans, A.J., Russell, A.J., Jóhannesson, T., Roberts, M.,
763 2015. A multi-dimensional analysis of pro-glacial landscape change at Sólheimajökull, southern
764 Iceland. *Earth Surface Processes and Landforms* 40:809-822.
- 765 Tarboton, D.G., 1997. A new method for the determination of flow directions and upslope areas in
766 grid digital elevation models. *Water Resources Research* 33: 309-319.
- 767 TauDEM (2016). TauDEM documentation - Utah State University.
768 <http://hydrology.usu.edu/taudem/taudem5/documentation.html> Last accessed October 2017.